Programmed cell death in the coccoid green microalga *Ankistrodesmus densus* Korshikov (Sphaeropleales, Selenastraceae)

Marcelo M. Barreto Filho, Pierre M. Durand, Nathan E. Andolfato, Anine Jordaan, Hugo Sarmento & Inessa L. Bagatini

View supplementary material
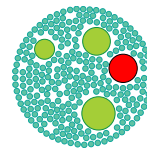
Published online: 23 Jul 2021.

Submit your article to this journal

Article views: 3

View related articles

View Crossmark data

British Phycological Society
Understanding and using algae

Taylor & Francis
Taylor & Francis Group

Check for updates

Programmed cell death in the coccoid green microalga *Ankistrodesmus densus* Korshikov (Sphaeropleales, Selenastraceae)

Marcelo M. Barreto Filho [a,b], Pierre M. Durand [c], Nathan E. Andolfato [a,b], Anine Jordaan [d], Hugo Sarmento [e] and Inessa L. Bagatini [a]

[a]Laboratory of Phycology, Department of Botany, Universidade Federal de São Carlos, São Carlos – SP, Brazil; [b]Post-graduate Program in Ecology and Natural Resources, Universidade Federal de São Carlos, São Carlos - SP, Brazil; [c]Evolutionary Studies Institute, University of the Witwatersrand, Johannesburg, South Africa; [d]Laboratory for Electron Microscopy, CRB, North West University, Potchefstroom, South Africa; [e]Laboratory of Microbial Processes and Biodiversity, Department of Hydrobiology, Universidade Federal de São Carlos, São Carlos – SP, Brazil

ABSTRACT

Reports of programmed cell death (PCD) across the taxonomic spectrum of photosynthetic unicellular organisms raise questions concerning its ecological and evolutionary roles. However, prior to ecological studies or evolutionary interpretations, it is essential to document phenotypic changes associated with PCD at the single-cell level, since death-related responses vary between taxa and within a single taxon depending on environmental stimuli. Here, we report responses to rapidly changing light, temperature and fluctuations in macronutrients in the model selenastracean green microalga *Ankistrodesmus densus* (Chlorophyta, Chlorophyceae, Sphaeropleales). We used stringent, but environmentally appropriate, conditions of prolonged darkness, nitrogen starvation (4 days), heat (1 h at 44°C) and cold shock (3 h at 2 ± 2°C). PCD phenotypes were examined by ultrastructural changes, phosphatidylserine (PS) externalization and DNA degradation. Flow cytometric Annexin V FITC analyses revealed that darkness and nitrogen-deprived cultures had significantly higher proportions of cells with PS externalization compared with controls ($p < 0.05$). Heat and cold treatments did not affect PS externalization ($p = 0.44$ and $p = 0.99$, respectively). Transmission electron microscopy (TEM) of light-deprived cells demonstrated, among other ultrastructural changes, marked cytoplasmic vacuolization suggesting a subtype of PCD known as vacuolar cell death. Nitrogen-starved cells had less vacuolization but presented more typical ultrastructural markers of PCD such as chromatin condensation and marginalization. In contrast, the more severe heat and cold shock treatments resulted in necrotic-like features. These findings suggest that prolonged darkness and nitrogen starvation induce PCD in a small (8.4 3.5 and 7.42 2.6%, respectively) but significant ($p < 0.05$) fraction of the *A. densus* population. Documenting these different death-related phenotypes depending on different environmental inducers is essential for interpreting ecological studies. Furthermore, our data support the hypothesis that autophagic/vacuolar cell death (VCD), which is central to organism homeostasis in plants (Streptophyta), occurs in Chlorophyta. VCD probably arose long before the evolution of multicellularity in plants.

HIGHLIGHTS

- Darkness and nitrogen deprivation induce different programmed cell death markers in *Ankistrodesmus densus*;
- Plant vacuolar-like cell death occurs in Chlorophyta;
- There is crossover between the vacuolar and apoptosis-like death morphotypes.

Introduction

Programmed cell death (PCD) can be loosely viewed as an active and genetically encoded self-destruction mechanism (Berman-Frank *et al.*, 2004; Bidle & Falkowski, 2004; Franklin *et al.*, 2006; Zuppini *et al.*, 2007). These active forms of cell death are important for embryonic development and maintenance of healthy adult tissues in multicellular organisms (Lockshin & Williams, 1964; Saunders, 1966; Leist & Nicotera, 1997; Jones, 2001). However, in unicellular organisms like phytoplankton our understanding of what PCD is, and its role in microbial ecology, is much more layered (Franklin *et al.*, 2006; Nedelcu *et al.*, 2011; Berges &

Choi, 2014; Bidle, 2015; Durand *et al.*, 2016). Indeed, the very term and 'the nature of programmed cell death' is a fraught question (Durand & Ramsey, 2019; Durand, 2020), but is central to our understanding of phytoplankton ecology and evolution (Segovia *et al.*, 2003; Franklin *et al.*, 2006; Berges & Choi, 2014; Bidle, 2015). Here we use the Berman–Frank *et al.*'s mechanistic definition of PCD as "active, genetically controlled, cellular self-destruction driven by a series of complex biochemical events and specialized cellular machinery" (Berman-Frank *et al.*, 2004). The evolutionary definitions are discussed elsewhere (Durand & Ramsey, 2019).

CONTACT Marcelo M. Barreto Filho ✉ barretof@uab.edu

Ecologically, the release of PCD products after cell death plays important intra- and interspecific ecological roles in phytoplankton populations and communities (Franklin et al., 2006; Vardi et al., 2007; Durand et al., 2011, 2014; Yordanova et al., 2013; Bidle, 2016). For example, PCD may impact others in the population by releasing signalling molecules and resources that either provide fitness benefits or coordinate population-level responses to environmental changes (Vardi et al., 2007; Durand et al., 2011, 2014; Yordanova et al., 2013). A variety of environmental triggers also lead to PCD in marine and freshwater communities affecting the biogeochemical flow of nutrients between and within trophic levels (e.g. Vardi, 2008; Orellana et al., 2013; Bidle, 2015, 2016). PCD also regulates the propagation and dispersal of colonial Trichodesmium spp. during unfavourable growth conditions (Berman-Frank et al., 2004), plays a role in community ecology (Orellana et al., 2013; Bidle, 2016), and was essential for the evolution of eukaryote cells and multicellular life (Michod & Nedelcu, 2003; Segovia et al., 2003; Blackstone, 2016; Durand et al., 2019).

Prior to interpreting the data on death in any ecological or evolutionary study, it is essential to document the environmental triggers and cell death morphotypes associated with PCD in a particular organism under specific conditions. Distinct markers and phenotypes reflect the organism's plasticity in adapting to environmental stresses (Bursch et al., 2006; Eisenberg-Lerner et al., 2009). Documenting the features of death in unicellular phytoplankton, however, can be challenging (Berges & Choi, 2014) and the distinction between death-related phenotypes has been a major problem (Jiménez et al., 2009; Berges & Choi, 2014). The reason for this is that researchers have used the methodologies imported from the multicellular world (Nedelcu et al., 2011; Proto et al., 2013) and what the results of the findings mean for unicellular organisms is not always clear (Berges & Choi, 2014; Durand, 2020). Results include morphological changes such as cell shrinkage, chromatin condensation and loss of phosphatidylserine (PS) membrane asymmetry, as well as biochemical markers like the activation of caspases (the caspase-metacaspase issue is discussed later) and DNA fragmentation (Bidle & Falkowski, 2004). In phytoplankton, however, a variety of morphologically and biochemically distinct morphotypes manifest in the same taxon upon different stimuli (Nedelcu, 2006; Jiménez et al., 2009; Sathe et al., 2019). Different taxa may also display different and unique markers even when the same stimulus is used (Affenzeller et al., 2009a; Vavilala et al., 2014). Comparing experimental data, therefore, requires one to know the morphotype associated with a specific scenario. In addition, typical mammalian assays are very sensitive, but not specific for detecting some PCD markers in unicellular organisms. The annexin-V assay, for example, that detects PS exposure,

can also be positive for other phospholipids (Weingärtner et al., 2012), whereas caspase assays may be positive in phytoplankton, even though they do not have orthologous mammalian caspases, but rather metacaspases (Uren et al., 2000; Aravind & Koonin, 2002; Tsiatsiani et al., 2011). Caspase-specific substrates correlate with metacaspase activity, but the results are not identical to those using a metacaspase-specific substrate (Spungin et al., 2019). The enzymes responsible for caspase activity in phytoplankton are currently unknown (for a recent review see Minina et al., 2020). As a consequence of the methodological complexities when documenting PCD, not all markers are observed within or between taxa in each cell death scenario. Experimental results can easily become conflated.

In metazoa, a classification of different PCD morphotypes has been proposed by the Nomenclature Committee on Cell Death (NCCD) (Galluzzi et al., 2012). Similar recommendations have been published for yeast (Carmona-Gutierrez et al., 2018) but a standardized nomenclature is missing for phytoplankton, even though there are many "different ways to die" (Jiménez et al., 2009), and differences in cell stress versus cell death responses (Mata et al., 2019). Autophagic-like cell death, for example, is associated with massive cytoplasmic vacuolization and is regulated by AuTophaGy- Related (ATG) and metacaspase (MCA) proteins (Tsujimoto & Shimizu, 2005; Duszenko et al., 2011; Minina et al., 2013, 2014a, b). This 'vacuolar' morphological subtype of PCD is an important death-related mechanism in higher plants but its presence in green phytoplankton is scarce. A related death morphotype was demonstrated in the streptophyte Micrasterias denticulata (Affenzeller et al., 2009b), and in the chlorophytes Chlamydomonas reinhardtii (Yordanova et al., 2013; Sathe et al., 2019), Dunaliella viridis (Jiménez et al., 2009) and Chlorella vulgaris (Papini et al., 2018). In autophagic/vacuolar death there is also crosstalk between autophagy and apoptosis mechanisms (Bursch, 2001; Bursch et al., 2006; Eisenberg-Lerner et al., 2009). Some of the markers of these PCD morphotypes overlap in phytoplankton depending on the nature and intensity of the stimuli (Affenzeller et al., 2009a, b). For consistency, throughout this manuscript we define autophagy as 'a process by which cells undergo partial autodigestion that prolongs survival for a short time under starvation conditions' (Tsujimoto & Shimizu, 2005). On the other hand, autophagic/vacuolar cell death (e.g. Affenzeller et al., 2009a, b; Jiménez et al., 2009), is 'mainly a morphological definition' (Tsujimoto & Shimizu, 2005) that represents a metacaspase-regulated switch from cell survival to PCD (Minina et al., 2014a, b). Therefore, 'autophagy' and 'autophagic/vacuolar cell death' have different evolutionary/ecology significance.

Among phytoplankton, chlorophytes are used extensively as model organisms to study PCD

(Berges & Choi, 2014; Bidle, 2015, 2016; Jiménez et al., 2009). Chlorophyta represent the biggest division of the 'green algae' comprising a great diversity of ubiquitous macro- and microalgae (Krienitz & Bock, 2012; Guiry & Guiry, 2020). Several chlorophytes have been investigated under a diverse range of environmental triggers, and many different cell death phenotypes have been described (Moharikar et al., 2006; Zuppini et al., 2007; Affenzeller et al., 2009a; Jiménez et al., 2009). They represent a valuable group in ecological and physiological studies of phytoplankton PCD.

Within the Chlorophyta, the asexual coccoid microalgae from the family Selenastraceae (Sphaeropleales, Chlorophyceae) comprise a highly diverse clade and are ubiquitous in inland waters (Krienitz & Bock, 2012; Garcia da Silva et al., 2017). They are particularly helpful as model organisms for PCD studies, particularly because there is no potential overlap between the induction of sexual reproduction and the PCD pathways, as observed in other green microalgae (Nedelcu et al., 2004) and plants (Kurusu & Kuchitsu, 2017). Despite being present in most freshwater ecosystems, little is known about how cell death programmes affect their ecophysiology (Franklin et al., 2006). Recently, evidence of PCD-like death was reported in Selenastraceae in a temperate eutrophic pond in the USA (Kozik et al., 2019) during the transition from spring to autumn. However, a correlation between changing conditions of irradiance, temperature and macronutrient fluctuations (e.g. N:C) and cell death was not identified (Kozik et al., 2019). Documentation of the ecological stimuli that may induce cell death and the associated death-related morphotypes in this important microalgal group is missing.

In this study, we report different modes of death in the common selenastracean green microalga *Ankistrodesmus densus* Korshikov (Chlorophyta, Chlorophyceae, Sphaeropleales) under rapidly changing conditions of light, temperature and fluctuations in macronutrients, all of which are ecologically relevant stimuli. PCD-related features can involve subtle markers. We have, therefore, used more stringent, but appropriate abiotic conditions to identify possible death-related morphotypes. These include total darkness, nitrogen deprivation, heat and cold shock.

Materials and methods

Model organism

The *Ankistrodesmus densus* (CCMA-UFSCar 3) strain used was isolated from a shallow tropical reservoir (Represa do Broa, Itirapina, SP, Brazil, 22°11′36.1″ S 47°53′24.1″W, isolated in 1979). CCMA-UFSCar 3 has been maintained in axenic conditions at the

Culture Collection of Freshwater Microalgae at the Universidade Federal de São Carlos, Brazil (CCMA-UFSCar, WDCM 835).

Cell culture

Ankistrodesmus densus CCMA-UFSCar 3 was cultured with a starting density of 1×10^4 cells ml^{-1} in WC medium, pH 7.0 (Guillard & Lorenzen, 1972), at 23°C (± 2°C), and 200 μmol photons m^{-2} s^{-1} under 12-12 h light-dark cycle. Cultures were agitated once a day. Prior to the experiments, the cultures were examined for bacterial and fungal growth in WC medium (pH 7) supplemented with peptone and glucose (250 mg l^{-1} each). No bacterial or fungal growth was observed on test tubes over 10 days.

For PCD assays, cells were harvested in the log-linear growth phase, which was determined from the average of three growth curves followed by *in vivo* chlorophyll *a* spectrophotometric measurements (HACH DR 5000) according to Griffiths et al. (2011) (Supplementary fig. S1). This is important, since cells should be healthy and young (as opposed to aged or dormant) in PCD experiments (Zhou et al., 2020).

Programmed cell death induction

Cells harvested in the log-linear phase were washed, counted using a hemocytometer and resuspended in sterile WC medium in 10 ml glass tubes to a final density of 1×10^6 cells ml^{-1}. Resuspended cells were subjected to four environmental stress treatments: prolonged darkness, nitrogen deprivation, heat and cold shock (experimental design in Supplementary fig. S2). No environmental stress was used in the controls. All treatments were performed in triplicate and were sampled and analysed at the same time.

For the nitrogen deprivation treatment, cells were washed three times using nitrogen-free WC medium at pH 7.0 before resuspension. Control and nitrogen-deprived cultures were incubated for 4 days under standard conditions, i.e. 23°C (± 2°C) and 12-12 h light-dark cycle at 200 μmol photons m^{-2} s^{-1}. For the dark-treated cultures, standard WC medium was used but cells were deprived of light for 4 days.

For the temperature treatments, cultures were maintained for 3 days under standard conditions pre-exposure to the shock conditions (a day before PCD measurements). For the heat shock, cell cultures were immersed in a water bath pre-heated to 44°C for 1 h and maintained under standard conditions for 16 h. A temperature of 44°C was chosen for comparison with earlier experiments using chlorophytes (Nedelcu, 2006; Durand et al., 2011, 2014) and because of the ecological relevance, since heat shock proteins were previously described in *Scenedesmus*

quadricauda (an *Ankistrodesmus* sister group) exposed to high temperatures (Zargar *et al.*, 2006). Cold shock was executed at 2 ± 2°C (cultures were placed in an ice bucket in a lighted fridge) for 3 h and retuned to standard conditions for 16 h. The cold shock temperature was motivated by earlier observations of chlorosis in *Chlorella* at 4°C (Tischner *et al.*, 1978), and from our unpublished observations of DNA fragmentation in *Chlamydomonas reinhardtii* when subjected to similar treatments. Strains of *Ankistrodesmus* may also be found in Antarctica (Kol & Flint, 1968) and temperate climes (Guiry & Guiry, 2020).

Programmed cell death analyses

The most informative assessment of PCD relies on integrating data from direct observation (e.g. TEM) with biochemical assays. To document PCD in *A. densus*, we used three markers: phosphatidylserine (PS) externalization with retention of membrane integrity, observation of PCD ultrastructural morphological changes, and DNA laddering. Other markers may be more sensitive but less specific (Durand, 2020) although of course they do provide information about what cellular responses are being induced. For example, caspase (Zhou *et al.*, 2020) and metacaspase (Mata *et al.*, 2019) activity can be associated with stress, but not necessarily with PCD.

Flow cytometry

PS externalization was detected by flow cytometry using the Apoptosis detection kit, BD Pharmingen, following the manufacturer's protocol. Briefly, 1×10^6 cells were harvested in log-linear phase, washed with PBS and resuspended in Annexin V binding buffer. From this suspension, approximately 1×10^5 cells were harvested by centrifugation and double-stained with annexin-V and propidium iodide (PI) for 15 min in the dark. Annexin V and PI positivity were assessed using a BD LSRFortessa™ cell analyzer (Becton-Dickinson, San Jose, California, USA) under the green FL1 (band-pass filter 530/30 nm) and orange FL2 (band-pass filter 575/26 nm) channels. The data were acquired using BD FACDiva software (flow rate = 31.54 µl min^{-1}; sample volume = 100 ul; voltage = 6.11), and analysed with the FlowJo software (10.5.3) as below.

For cytometric analyses, the autofluorescence of chlorophyll in control cells (unstained) in the FL3 channel was extremely high (> 10^5) even with voltages set at a lower gain. This was largely overcome by reading PI in the FL2 channel, which 'does not capture the longer autofluorescent wavelengths of *C. reinhardtii*' (see channels D and E in table 1 in Kay *et al.*, 2013), and is unlikely to interfere with the

PI signals. The transition across the spectrum of PCD was determined previously (Carmona-Gutierrez *et al.*, 2010, 2018; Kay *et al.*, 2013; Durand *et al.*, 2014). Healthy cells are FITC-Annexin V negative (FITC-) and PI negative (PI-) (quadrant 4); early PCD cells are FITC-Annexin V positive (FITC+) and PI negative (quadrant 3); late PCD cells FITC-Annexin V positive and PI positive (PI+) (quadrant 2); finally, necrotic lysed cells are PI positive only (quadrant 1).

Although ideal, compensation for fluorescence spillover between channels was not performed because it was unclear what the positive controls for phytoplankton should be (Gasol & Morán, 2015). Cytograms were analysed with FlowJo (v10.5.3) with a minimum of 1×10^4 cells acquired for each sample (n = 3). Populations were gated using SSC versus FSC two-dimensional dot plots (Kay *et al.*, 2013; Durand *et al.*, 2014; Satpati *et al.*, 2016). The FL3 channel, which is commonly used in flow cytometry studies of chlorophytes, was intentionally avoided because it excludes dead (i.e. late PCD or necrotic) cells.

Statistical analyses were performed with R (v4.0.2). A low proportion of PS externalization and high variability in annexin-V positive cells was noted. Therefore, the Annexin-V and PI datasets were log-transformed (as suggested by Dingman & Lawrence, 2012) to obtain normal distributions. The assumptions of homogeneity of variance and normal distribution were assessed using the Shapiro–Wilk normality test (Supplementary table S1) and Levene's homogeneity test, respectively (Supplementary table S2). The outcome of FITC+ (early PCD) and FITC+ PI+ (late PCD) passed the normality test, but PI+ (detects membrane damage) failed. For data with normal distribution (FITC+ and FITC+ PI+) the percentage of annexin V binding cells in controls was compared with treated cultures using one-way analysis of variance (ANOVA). Comparisons were performed using the R package multcomp (Hothorn *et al.*, 2008) with a Dunnet's multiple-comparison post-test (Supplementary table S3). For the ANOVA analyses, the assumption of normality of residuals was confirmed with the Shapiro–Wilk normality test (Supplementary table S4). For the PI variable, we proceeded with the alternative Kruskal–Wallis test (Supplementary table S5).

Transmission electron microscopy (TEM)

Cell samples were fixed for 4 h at room temperature (20–25°C) with 2% glutaraldehyde in 0.025 sodium cacodylate buffer (pH 7.5). Three ml of each cell suspension from each biological replicate was pooled. For the control and each experimental sample, 9 ml was added to an equal volume of 4% glutaraldehyde in 0.05 M sodium cacodylate buffer (pH 7.5) (Nozaki *et al.*, 1994). Samples were washed 3 times in 0.025 M sodium cacodylate buffer and pelleted using an IKA mini G centrifuge at

$3000\times g$. Cell pellets were post fixed with 2% osmium tetroxide in 0.025 M sodium cacodylate buffer for 2 h at room temperature followed by two washes with 0.025 M sodium cacodylate buffer. The fixed materials were then dehydrated for 10 min each in 5, 10, 25, 40, 70, 80, 95 and 100% ethanol followed by a final dehydration in 100% ethanol for 20 min. After dehydration, cells were transferred to increasing ethanol-LR White resin ratios of 3:1; 2:1; 1:1 for 20 min each, then twice in 100% LR White resin for 45 min each and finally left overnight at 4°C. The following day, cells were embedded in fresh LR White resin in gelatin capsules and allowed to polymerize at 65°C. The hardened resin blocks were sectioned at 90 nm thickness with an ultramicrotome (Ultracut E, Reichert-Jung, Vienna, Austria) and the sections were collected on copper grids (5–10 grids per sample; each grid had several thin sections). Grids were stained with 5% aqueous uranyl acetate and lead citrate (Reynolds, 1963), dried and examined with a FEI Tecnai G2 Transmission Electron Microscope at 120 kV. TEM micrographs were taken randomly along different fields of view (FOVs) and the following ultrastructural changes documented: vacuolization, chromatin condensation, chloroplast disruption, mitochondrial disruption (elongation and swelling), and shrinking of the protoplasm. Results of the above markers were summarized in a presence-absence (binary) matrix, where each cell presented a different ID. Frequency (number of micrographs) and relative abundance of each condition for each treatment were performed in using R v4.0.2 using the package tidyverse (Wickham *et al.*, 2019) (Supplementary table S6; Supplementary fig. S3). Relative abundance was assessed by dividing the frequency by the total number of cells analysed in each treatment.

DNA fragmentation

DNA laddering is considered a specific, but not necessarily sensitive, measure of PCD (Durand, 2020). Biological replicates for each treatment and the control were pooled (giving a total of 9 ml) to increase the chances of detection. Cell suspensions were centrifuged,

and the genomic DNA was extracted following the manufacturer's protocol of the DNeasy Powersoil kit (Qiagen). Agarose gel electrophoresis was performed with the isolated DNA (1% agarose gel; 45 min; 80V).

Results

Loss of membrane asymmetry and membrane integrity

Flow cytometric analysis of PS externalization (FITC+ only) revealed that the darkness and nitrogen starvation treatments were significantly different from the control cultures (ANOVA test, $p < 0.001$; Dunnet's test, $p < 0.05$, n = 3, Supplementary table S3, Fig. 1a). Temperature (heat and cold) shock treatments did not affect PS externalization significantly (Dunnet's test, $p = 0.44$ and $p = 0.99$, n = 3, respectively, Fig. 1a). In light-limited and nitrogen-starved cultures, respectively, 8.4 ± 3.5 and 7.42 ± 2.6% of the cells showed PS externalization, while in the control, heat and cold stressed cultures, respectively, 2.9 ± 0.3, 2.1 ± 0.4 and 3.1 ± 0.5% of the cells showed this PCD phenotype (Q3 in Fig. 2).

For FITC and PI double positive, in the nitrogen-deprived treatment 8.29 ± 1.7% of cells detected positive, but this was not significantly different (ANOVA test, $p = 0.29$, n = 3, Fig. 1b) from the control (4.45 ± 0.9%). However, quadrant 2 provides less information about the mode of death, since cells positive for both FITC Annexin V and PI could have died by either an apoptosis-like pathway or as a result of a necrotic process.

In contrast, heat-shocked cells (15.6 ± 4%) demonstrated membrane permeabilization (PI+ only) compared with 5.42 ± 1.7%, 5.27 ± 1 and 6.49 ± 1.3% in the control, dark and nitrogen treatments, respectively (Q1 in Fig. 2). Although the heat-shock cultures had a much higher mean relative to the control cultures for PI+ (Fig. 1c), the variability between replicates may have prevented results being statistically significant (Kruskal–Wallis test, $p = 0.067$, n = 3, Supplementary table S5, Fig. 1b). It is noted that if we had considered ANOVA sufficiently robust to moderate variations to
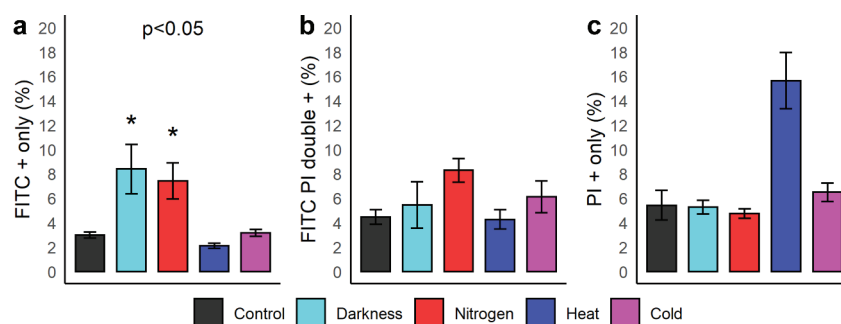

Fig. 1. PCD and cell viability assessment of *Ankistrodesmus densus* after exposure to the Darkness, Nitrogen deprivation, Heat and Cold treatments. (**a**) Percentage of cells positive for Annexin V FITC. (**b**) Percentage of cells positive for FITC and PI. (**c**) Percentage of cells positive for PI. Asterisk (*) marked values = statistically significant ($p < 0.05$, n = 3).
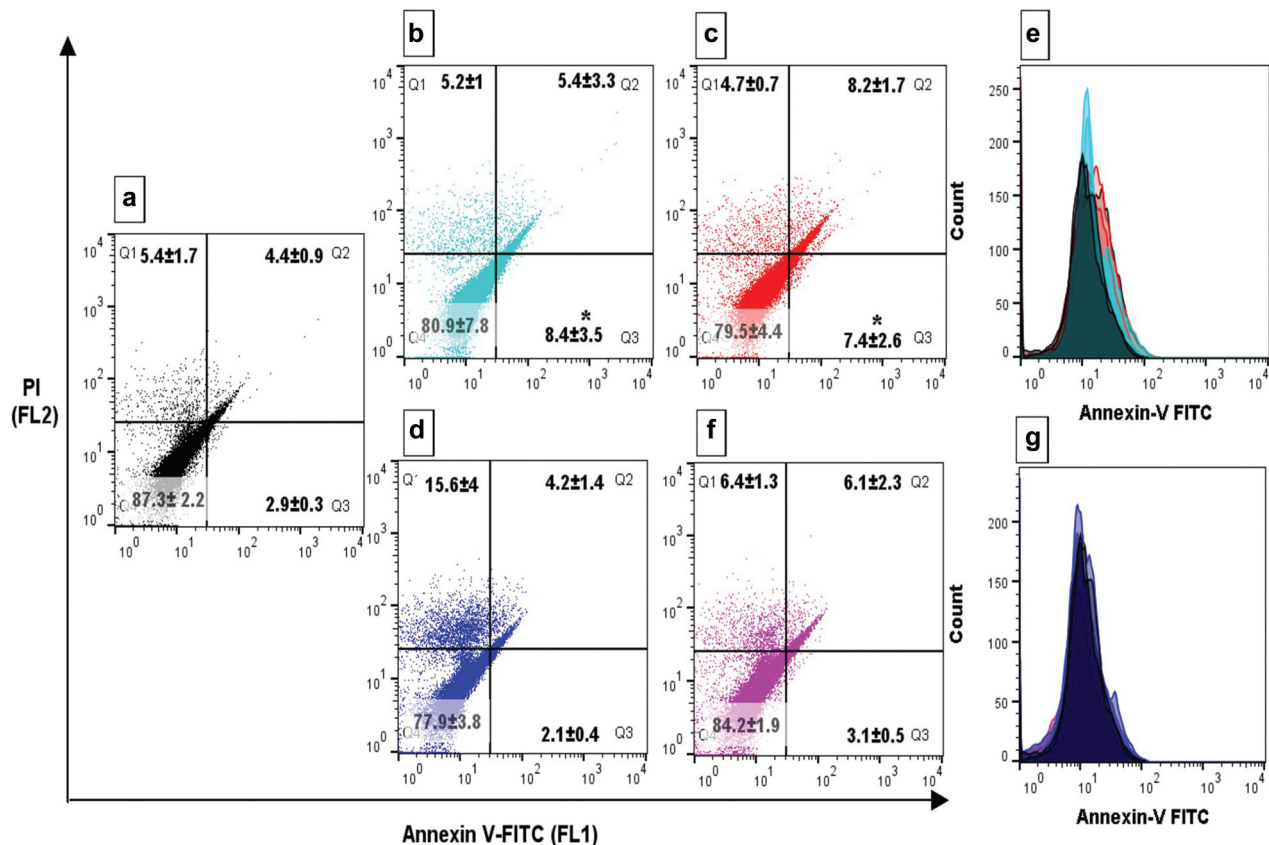
Fig. 2. PCD flow cytometric detection in *A. densus*. (**a**) to (**e**) are dot-plots of samples (10 000 cells each), in triplicate, of the Control, Darkness, Nitrogen deprivation, Heat and Cold treatments, respectively. The x axes represent the FITC fluorescence and the y axes the PI fluorescence. Q1 = includes necrotic cells (PI + and FITC− cells); Q2 = includes late PCD cells (FITC + and PI + cells); Q3 = includes early PCD cells (FITC + and PI− cells) and Q4 = includes healthy cells (FITC− and PI− cells). (**f**) Overlapped histograms of the control, darkness, and nitrogen starvation treatments. (**g**) Overlapping histograms of the control, heat and cold shock treatments. The average percentage value and the standard deviation in each of the four quadrants (Q1, Q2, Q3 and Q4) for each of the four environmental stimuli is indicated. Asterisk (*) marked values = statistically significant ($p < 0.05$, n = 3).

normality (as suggested by Blanca *et al.*, 2017), a significant result would have been obtained (ANOVA test = $p < 0.001$, Dunnet's test, $p < 0.05$, n = 3, Supplementary table S7).

The higher proportion of cells bound to FITC-Annexin V (FITC+ only) in darkness and nitrogen-depleted treatments can also be seen in the histograms (Fig. 2f) as a small shift to the right when superimposed over control cultures. In contrast, heat and cold treatments showed complete overlapping of the control histogram (Fig. 2g).

Ultrastructural changes by transmission electron microscopy (TEM)

Ultrastructural micrographs of *A. densus* cells growing actively in control cultures (Figs 3–6) showed a large nucleus with a central nucleolus surrounded by uncondensed chromatin (Fig. 6); one parietal chloroplast with regularly organized thylakoid membranes (Figs 4 5); and a dense homogeneous cytoplasm with mitochondria (Fig. 4). Except for some

mild cytoplasmic vacuolization (relative abundance = 0.2, Supplementary fig. S3a), control cells did not contain any of the other PCD-associated features.

In comparison to control cultures, the dark-treated cultures (Figs 7–10) underwent marked cytoplasmic vacuolization (relative abundance = 0.71, Supplementary fig. S3a), with each vacuole containing electron-dense materials (Figs 7–9, arrows labelled 1). In dark-treated cultures, many mitochondria, chloroplasts, plasma and nuclear membranes remained intact, but mitochondrial elongation (Figs 8 and 9, arrows labelled 4) was eventually observed (relative abundance = 0.14, Supplementary fig. S3d). A single mass of chromatin condensation (pyknosis) was noted in the centres of the nuclei in some cells, but no marginalization could be seen (Fig. 10, arrow 2).

Nitrogen-starved cells (Figs 11–14) exhibited cytoplasmic vacuolization (Fig. 11, arrows 1; relative frequency = 0.55, Supplementary fig. S3a), but less than that observed in light-deprived cells. Unlike the dark treatment, however, these cells presented photosynthetic membrane impairment and disruption of the
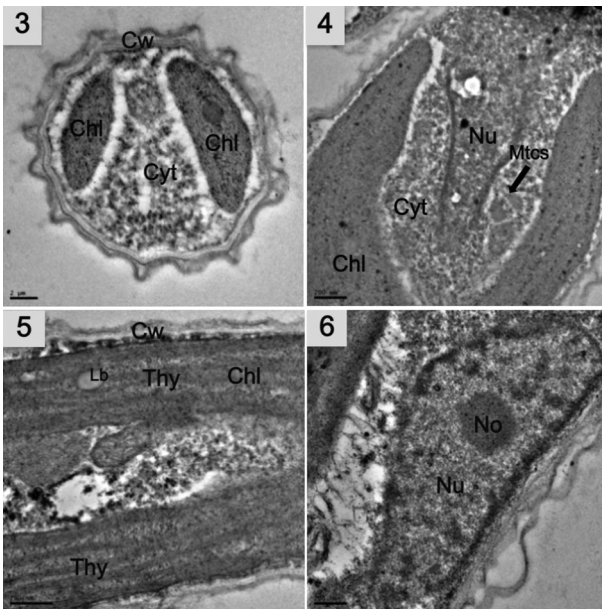
Figs 3–6. Normal vegetative cells actively growing on WC in control conditions. Note the cytoplasm without vacuolization. Nu, nucleus; No, nucleolus; Mtc, mitochondria; Cw, cell wall; Cyt, cytoplasm; Chl, chloroplast; Thy, thylakoid. Scale bars: **Fig. 3**. 2 μm; **Figs 4–6**. 0.2 μm.
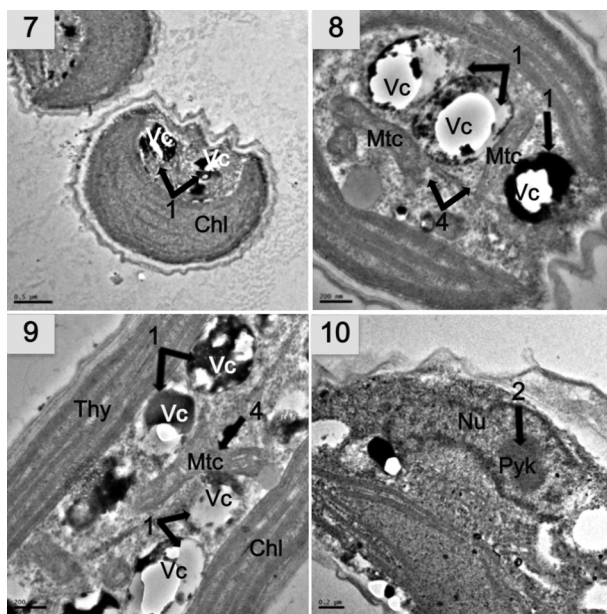
Figs 7–10. Cells after 4 days in darkness. There is extensive cytoplasmic vacuolization (arrows 1), mitochondrial elongation (arrows 4), and chromatin condensation (pyknosis) without chromatin marginalization (arrow 2). Vc, Vacuole; Pyk, Pyknosis; Chl, Chloroplast; Mtc, Mitochondria; Thy, Thylakoid. Scale bars: **Fig. 7**. 0.5 μm; **Figs 8–10**. 0.2 μm.

typical stacked thylakoid membrane structure (relative frequency = 0.22, Supplementary fig. S3c, Figs 11 and 12, arrows labelled 3) by electron-lucent ('empty') spaces between the thylakoids. This has been observed previously (Zuppini *et al.*, 2007; Zhou *et al.*, 2020). We also noted a structure that resembled a plastid with blebbing (Supplementary fig.

S4). Adjacent vacuoles presented electron-dense materials (Supplementary fig. S44, black arrow). Although unclear, the internal tortuous structures resemble double membranes, and might possibly be highly disorganized thylakoids (Supplementary fig. S4a, white arrows). Mitochondrial elongation was not observed. The relative frequency of chromatin condensation was 0.22 (Supplementary fig. S3b). Specifically, nucleolar shrinkage/condensation and movement of the chromatin to the nuclear membrane was detected (Fig. 13, arrows labelled 2), resulting in chromatin marginalization (Fig. 14, arrows 2).

Heat-shocked cultures (Figs 15–18) exhibited a lower relative abundance of vacuolization compared with dark or nitrogen-deprived treatments, and only marginally higher compared with the controls (Figs 16 and 17, arrows labelled 1; relative abundance = 0.33, Supplementary fig. S3a). In contrast to the controls, however, some cells exhibited shrunken, damaged protoplasm with membrane detachment from the cell wall (Figs 15–16, arrows 5; relative abundance = 0.25, Supplementary fig. S3e). Complementing the PI+ flow cytometry data (Q1 in Fig. 2), TEM micrographs revealed possible areas of membrane rupture (Fig. 15, arrow 5), although this is difficult to ascertain. Evidence of thylakoid membrane impairment was noted (Fig. 17, arrows 3), although at a much lower frequency (relative frequency = 0.08, Supplementary fig. S3b) compared with nitrogen-deprived cells. Mitochondrial disruptions were very rarely observed in heat-shocked cultures, but at least one cell presented a mitochondrion with a 'balloon-shaped' membrane protrusion at one pole (see Supplementary fig. S4b).

Cold-shocked cells did not exhibit cytoplasmic vacuolization (relative abundance = 0.09, Supplementary fig. S3a). Mitochondrial disruption was reported (relative abundance = 0.27, Supplementary fig. S3d) with the 'swollen' phenotype (Figs 20 and 22, arrows 4) as opposed to the 'elongated' abnormality seen in the dark treatment. Chromatin condensation occurred in the cold-shock treatment (Fig. 22, arrow 2; relative frequency = 0.18, Supplementary fig. S3b), but without chromatin marginalization. Only discrete electron-lucent spaces were seen between thylakoids (Fig. 21, arrow 3). Shrinkage of the protoplasm was noted (Fig. 19, arrows 5; relative frequency = 0.18, Supplementary fig. S3e).

DNA fragmentation

Neither the control nor the stressed cells displayed DNA laddering by gel electrophoresis (Supplementary fig. S5).

Discussion

The aim of this study was to investigate PCD phenotypes in the common selenastracean green alga
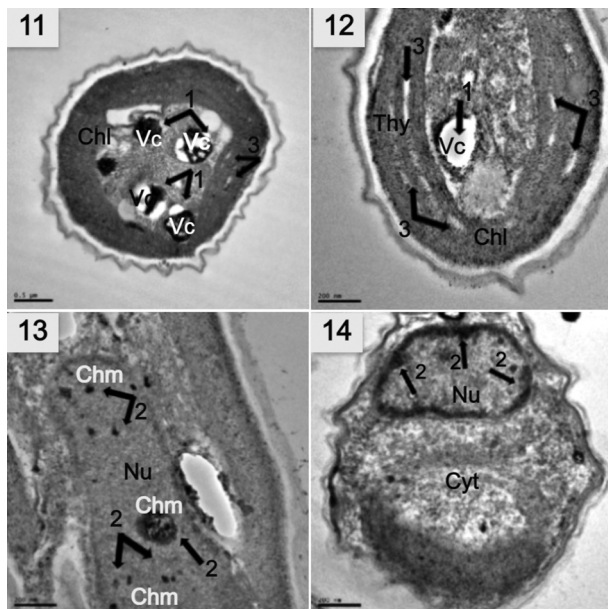
Figs 11–14. Cells after 4 days with nitrogen deprivation. Cells exhibited vacuolization (arrows 1) and chloroplast disruption (arrows 3). There was nucleolar condensation and movement of chromatin to the nuclear membrane (arrows 2) with marginalization. Vc, Vacuole; Chl, Chloroplast; Chm, Chromatin; Nu, nucleus; Cyt, Cytoplasm. Scale bars: **Fig. 11**. 0.5 μm; **Figs 12–14**. 0.2 μm.
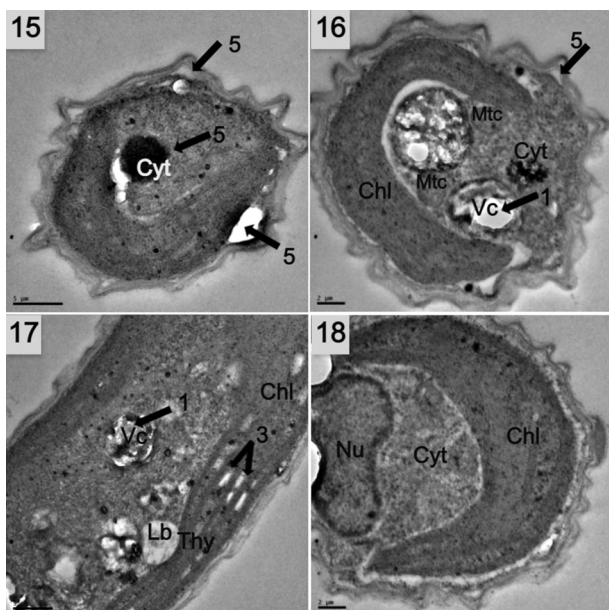
Figs 15–18. Cells after exposure to 44°C for 1 h and returned to standard conditions for 16 h. A shrunken, damaged protoplasm and membrane detachment from the cell wall were noted (arrows 5). There were disrupted thylakoids, indicated by the 'white' spots (arrow 3). Cytoplasmic vacuolization was observed although much less than that observed in the Darkness and Nitrogen deprivation treatments (arrows 1). Scale bars: **Fig. 15**. 5 μm; **Fig. 16**. 2 μm; **Fig. 17**. 5 μm; **Fig. 18**. 2 μm.

A. densus. These data are essential for interpreting the results from evolutionary ecology studies in the

family Selenastraceae. We exposed this alga to the ecologically relevant stresses of darkness, nitrogen deprivation, heat and cold. Our results indicate that darkness and nitrogen deprivation induce specific PCD phenotypes. The marked cytoplasmic vacuolization is an important and noteworthy morphotype in this model organism.

Reports of PCD in Selenastraceae, a ubiquitous group, are rare. One of the very few reports is by Kozik *et al.* (2019), who identified a link between cell death and a mixture of abiotic and biotic factors. Although the authors did not find a correlation between thresholds of irradiance, temperature, and nitrogen fluctuations and the PCD phenotype, here we show that environmental disturbances can induce markers of PCD in *A. densus*. In natural conditions, some green microalgae experience periods of prolonged darkness (e.g. La Rocca *et al.*, 2015). *Scenedesmus acuminatus* populations, for instance, can survive up to 4 months in complete darkness in Antarctica (Dehning & Tilzer, 1989). Similarly, under natural conditions, nitrogen-deprived *Chlamydomonas* cells produce H_2O_2 (Philipps *et al.*, 2012), which is an inducer of PCD in chlorophytes (Murik *et al.*, 2009, 2014; Vavilalla *et al.*, 2015). In *Chlamydomonas reinhardtii* the overlap between nitrogen starvation and PCD is conclusive (Sathe *et al.*, 2019).

After 4 days in complete darkness, *A. densus* cells had a statistically significant result for Annexin V FITC only (Fig. 1a) indicating that a small but significant proportion of the population underwent PCD (8.4 ± 3.5%). This number is in agreement with a cell death seasonal pattern study of 19 phytoplankton species, which noted that the proportion of cells staining positive for annexin V in nature ranges from 2% to nearly 30% (Kozik *et al.*, 2019). The range may reflect the relatively short window for sampling, when cells are in the early apoptosis-like period and FITC+ and PI- (Kozik *et al.*, 2019). One point worth noting is that while chlorophytes have been repeatedly shown to bind Annexin V (Moharikar *et al.*, 2006; Segovia & Berges, 2009; Orellana *et al.*, 2013; Durand *et al.*, 2014), PS is not present in some green algal taxa (Giroud *et al.*, 1988). The positive results appear to be due to the affinity of Annexin V for other membrane phospholipids like phosphatidylethanolamine (PE) and phosphatidylglycerol (PG) (Weingärtner *et al.*, 2012). This may have the same significance for PCD but phospholipid relative abundance in *Ankistrodesmus* has not been assessed.

The most striking TEM finding in light-deprived cells is the massive cytoplasmic vacuolization which included electron-dense material (relative abundance = 0.71). This degree of cytoplasmic vacuolization has been described before in chlorophytes (Affenzeller *et al.*, 2009a, b; Jiménez *et al.*, 2009; Yordanova *et al.*, 2013; Sathe *et al.*,
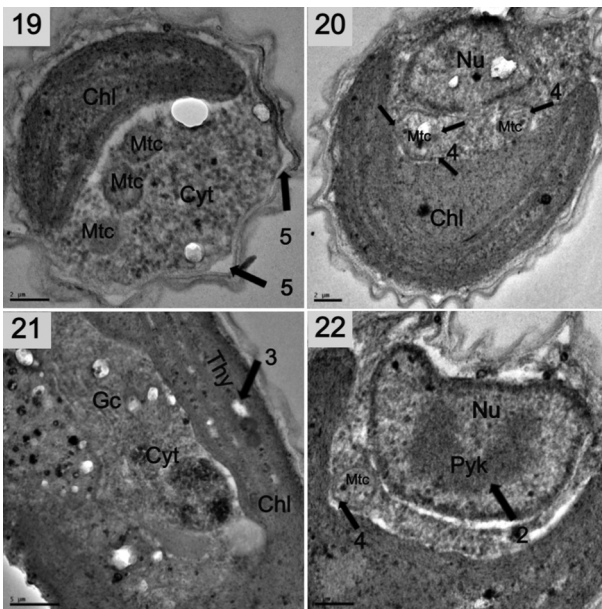
Figs 19–22. Cells after exposure to cold shock (2 ± 2°C) for 3 h and standard growth conditions for 16 h. There was very little vacuolization (not shown in the panels), however, deformed 'swollen' mitochondria (arrows 4), shrinking of the protoplasm (arrows 5), and slight disruption between the thylakoids were observed (arrow 3). Chromatin condensation could be seen (arrow 2). Scale bars: **Fig. 19**. 2 μm; **Fig. 20**. 2 μm; **Fig. 21**. 5 μm; **Fig. 22**. 2 μm.

2019), cyanobacteria (Ning *et al.*, 2002; Berman-Frank *et al.*, 2004; Zhou *et al.*, 2020), social amoebae (Cornillon *et al.*, 1994; Otto *et al.*, 2003), vascular plants (Danon *et al.*, 2000; van Doorn *et al.*, 2011), as well as mammals (Henics & Wheatley, 1999). This phenotype is typical of vacuolar/autophagic cell death, a distinct form of PCD (Bursch *et al.*, 2006; Afenzeller *et al.*, 2009*a, b*), and may also involve pyknosis (Bursch, 2001), which we noted in some cells (Fig. 10, arrow 2). The chromatin condensation associated with pyknosis is similar to that observed in nitrogen-starved *Dunaliella viridis* (Jiménez *et al.*, 2009) and *Chlamydomonas reinhardtii* (Sathe *et al.*, 2019) cells and is distinct from the well-defined nucleolus observed in actively growing *A. densus* (Fig. 6). The appearance of elongated mitochondria is suggestive of autophagy (Figs 8, 9, arrows 4). During autophagy, mitochondria may fuse and elongate, which protects against degradation and leads to greater cellular energy (ATP content) (Gomes & Scorrano, 2011; Gomes *et al.* 2011). This supports Minina *et al.*'s hypothesis that autophagy has both cytoprotective and cytotoxic roles during the execution of vacuolar PCD (Minina *et al.*, 2014*a, b*). The ATP content is key in mediating PCD (Zhou *et al.*, 2020), and autophagy may be essential to maintain the energy status of dying cells (Minina *et al.*, 2014*a, b*). Cytoplasmic vacuolization and mitochondrial swelling may also be found in paraptosis (Sperandio *et al.*, 2000; Franklin & Berges, 2004), however in our light-deprived cells chromatin condensation was found and this is not classified as a feature of paraptosis (Sperandio *et al.*, 2000). Further

investigation is required to explore the possible involvement of ATG proteins in *A. densus* cell death.

The relative frequency of 0.71 (Figs 7–10, arrows labelled 1) indicates that vacuolization is widespread in the population, even while the flow cytometric findings suggest a much lower proportion of cells undergoing PCD. This discrepancy may be related to the different sample sizes of TEM and flow cytometry (n = 10,000 cells for flow cytograms), or to the different sensitivities of the two measures. PS is usually interpreted as a marker of apoptosis-like forms of death, although on some occasions it can be associated with autophagic cell death (Eisenberg-Lerner *et al.*, 2009). The presence of vacuolization and PS externalization supports the notion that apoptotic-like and autophagic-like cell death processes should not be seen as 'mutually exclusive phenomena' (Bursch, 2001; Lockshin & Zakeri, 2004; Bursch *et al.*, 2006). Rather the crosstalk between both cell death morphotypes depends on the stimulus and the cellular context (Bursch *et al.*, 2006; Maiuri *et al.*, 2007; Eisenberg-Lerner *et al.*, 2009). The overlap between autophagic/vacuolar-like and apoptosis-like PCD has previously been observed in chlorophytes (Affenzeller *et al.*, 2009*a, b*; Jiménez *et al.*, 2009; Yordanova *et al.*, 2013) and yeast (Carmona-Gutierrez *et al.*, 2010). The reason for the lack of DNA fragmentation is not clear. While DNA laddering is a known feature of the more typical apoptotic-like morphotype of PCD in chlorophytes (Moharikar *et al.*, 2006; Nedelcu, 2006; Durand *et al.*, 2014), it is not reported consistently (Leu & Hsu, 2005; Zuppini *et al*, 2007).

These findings have some significance for the evolutionary ecology of PCD en route to multicellularity in plants. In higher plants, metacaspase-dependent autophagy plays a prominent role in triggering 'vacuolar cell death (VCD)' (van Doorn *et al.*, 2011; Minina *et al.*, 2013, 2014*a, b*), by mechanisms that 'sequester cellular components en masse and deliver them into the vacuole for degradation' (Minina *et al.*, 2014*b*). VCD – as opposed to other PCD mechanisms like apoptosis – occurs in plants, presumably because of their rigid cell walls, which prevent the fragmentation of the cells into membrane-bound apoptotic bodies (van Doorn *et al.*, 2011). VCD has implications for plant development (van Doorn *et al.*, 2011; Hara-Nishimura & Hatsugai, 2011; Minina *et al.*, 2013, 2014*a*) and in the pathogen-triggered hypersensitive response (Jones, 2001; Hofius *et al.*, 2011), but how exactly VCD-associated metacaspases crosstalk with the autophagy machinery to regulate other plant physiological functions (e.g. 'senescence-associated vacuoles' induced by stress factors (Carrión *et al.*, 2013; Costa *et al.*, 2013)) remains unclear (Minina *et al.*, 2014*b*, 2017). Intriguingly, some of the reports of PCD in unicellular green microalgae are of the autophagic/vacuolar cell death

kind. For example, VCD has been observed in the 'charophyte' *Micrasterias denticulata* (Affenzeller *et al.*, 2009a, b), and in the chlorophytes *Chlamydomonas reinhardtii* (Yordanova *et al.*, 2013; Sathe *et al.*, 2019) and *Dunaliella viridis* (Jiménez *et al.*, 2009). In metal-stressed Chlorellaceae (Chlorophyta), autophagic activity led to widespread vacuolization and an accumulation of electron-dense material (Papini *et al.*, 2018) very similar to those observed in *A. densus* in this study. The green algae comprise Chlorophyta (which includes *A. densus*) and Streptophyta, which includes both algae ('Charophyta') and plants (Embryophyta) (Lewis & McCourt, 2004; Leliaert *et al.*, 2012). The documentation of vacuolar-like cell death in cell-walled *A. densus* supports Segovia *et al.*'s assertions that key elements of cell death pathways arose earlier in unicellular chlorophytes and were subsequently appropriated by higher plant lineages through the course of evolution (Segovia *et al.*, 2003). Of course, we cannot rule out that *A. densus* acquired this form of cell death independently of the streptophytes, but the evidence for similar PCD-related cytoplasmic vacuolization in other chlorophytes as well as streptophytes suggests a shared, earlier origin of VCD.

Nitrogen-starved *A. densus* cells demonstrated ultrastructural apoptotic-like hallmarks such as the movement of condensed chromatin from the nucleolus to the nuclear membrane (Figs 13–14, arrows 2), pyknosis and the margination of chromatin (Fig. 14, arrow 4). These observations have been noted in other chlorophytes (Segovia *et al.*, 2003; Zuppini *et al.*, 2007; Jiménez *et al.*, 2009). Our nitrogen-starved cells also exhibited a small but statistically significant positive result for PS exposure (7.4%) and retention of plasma membrane integrity (Fig. 1a, c). Because these cultures also exhibited cytoplasmic vacuolization, which is the hallmark of VCD, we support the claim that there is crosstalk between apoptosis-like and vacuolar/autophagic cell death mechanisms in the Selenastraceae. This observation also corroborates the view that autophagic and apoptosis-like PCD can act in a cooperative manner to determine the cell's fate in a particular ecological scenario (Maiuri *et al.*, 2007; Carmona-Gutierrez, 2010).

DNA laddering (a marker of apoptosis-like PCD) was not seen in nitrogen-depleted cultures. The absence of DNA laddering has been noted before, for example, heat-stressed *Chlorella sacharophila* undergoing PCD also demonstrated chromatin marginalization and chloroplast alterations without visible DNA laddering (Zuppini *et al.*, 2007). The disruption of the regular thylakoid structure might be a direct effect of N-deprivation, although similar electron-lucent spots have been seen elsewhere when PCD-related phenotypes were reported (e.g. Zuppini *et al.*, 2007; Sathe *et al.*, 2019; Zhou *et al.*, 2020). The nature of this electron-lucent material is currently unknown.

Exposure of cells to heat shock resulted in a shrunken damaged protoplasm with detachment of the plasma membrane from the cell wall (Figs 15–16, arrows 5). A few cells also presented empty spaces between the thylakoids, which may suggest a partial dismantling of the chloroplast structure (Fig. 17, arrows 3). Similar features have been identified as PCD in other green algae like *Chlorella* (Zuppini *et al.*, 2007), but the non-significant annexin-v FITC+ only data in conjunction with the much higher percentage of PI+ heat-treated cells (Fig. 1C; see also Supplementary table S7) suggest that these alterations may be due to the physical effects of heat within cells itself as opposed to PCD. Although there is no clear-cut parameter that allows the separation of PI-only positive and PI and FITC double positive subpopulations, any event that falls in the Q1 quadrant was interpreted as primary necrotic non-PCD cells (Carmona-Gutierrez *et al.*, 2010, 2018). Indeed, the balloon-shaped protrusion of the mitochondrial membrane (Supplementary fig. S4b), although very rarely observed here, has been seen in *M. denticulata* and it has been argued that this ultrastructural feature is due to the abiotic stress itself rather than functional regulation (Affenzeller *et al.*, 2009a, b).

Cold-treated cells did not show any significant annexin V FITC and PI staining when compared with the controls. The chromatin condensation observed was similar to that seen in nitrogen-deprived cells (Supplementary fig. S3), although no marginalization was seen. These moderate non-marginal chromatin clusters (Fig. 22, arrow 2) can occasionally occur during necrosis (Kroemer *et al.*, 2009; van Doorn *et al.*, 2011; Hou *et al.*, 2016). The higher percentage of 'swollen', disrupted mitochondria and protoplasm shrinkage in cold cultures (Figs 20, 22, arrows 4) compared with the dark and nitrogen-deprived cultures may be due to the physical effects of the cold shock itself, since there was no other evidence of PCD-related ultrastructural changes.

Natural systems are fundamentally different from laboratory unialgal cultures. Although in nature many other factors are likely to play a role in selenastracean losses (Kozik *et al.*, 2019), this study provides a link between ecologically relevant stimuli like prolonged darkness and nitrogen deprivation and PCD. Our results describe the specific markers and morphotypes associated with PCD studies in Selenastraceae, which will be important for future cell death work in this model lineage. We also demonstrate an interplay between autophagic and apoptotic-like features, supporting the notion that these mechanisms are not mutually exclusive.

Coetzer from the School of Pathology both at the University of Witwatersrand, Johannesburg, South Africa, for kindly providing their laboratory facilities and some materials and reagents. We also thank Karen van Niekerk for assistance with the flow cytometry experiments. We are also grateful to Prof. Armando Vieira, Prof. Odete Rocha, Prof. James Jeffrey Morris and Dr. Thaís Garcia for valuable comments and suggestions.

Disclosure statement

No potential conflict of interest was reported by the author(s).

Supplementary information

The following supplementary material is accessible via the Supplementary Content tab on the article's online page at https://doi.org/10.1080/09670262.2021.1938240

Supplementary fig. S1. Growth curve of Ankistrodesmus densus under standard growth conditions (see text for more details). The black arrow indicates the day when cells were harvested for the assays of PCD induction.
Supplementary fig. S2. Experimental design for the experiments performed.
Supplementary fig. S3. The relative abundance of each characteristic marker under exposure to standard conditions (control), darkness, nitrogen deprivation, heat and cold shock. Raw data is included in table S6. chm = chromatin; chl = chloroplast; mit = mitochondria; prot = protoplasm.
Supplementary fig. S4. Additional TEM micrographs showing (a) a structure that could be highly disorganized thylakoids (white arrows). The black arrow indicates the electron-dense material inside the vacuoles. (b) A mitochondrion with 'balloon'-shaped membrane protrusion (black arrow).
Supplementary fig. S5. Agarose gel electrophoresis (1% agarose, 45 min, 80V) of genomic DNA extracted from cultures under control standard conditions, darkness, nitrogen deprivation, heat and cold shock. No fragmentation could be observed.

Supplementary table S1. Shapiro–Wilk test for normality assessment.
Supplementary table S2. Levene's homogeneity for assessment of homogeneity of variances.
Supplementary table S3. Dunnet's multiple-comparison post-test fitting the ANOVA with FITC as the outcome variable.
Supplementary table S4. Shapiro–Wilk test for the assessment of normality of the residuals in the ANOVA model with FITC+ and FITC+ PI+ as the outcome variables.
Supplementary table S5. Kruskal–Wallis test for the comparison of means with PI as the outcome variable.
Supplementary table S6. The frequency and relative abundance for each marker under the different treatments. N = number of cells analyzed per treatment; ƒ positive = presence of the marker; ƒ negative = absence of the marker; rel. abundance positive (%) = ƒ positive divided by N; rel. abundance negative (%) = ƒ negative divided by N.
Supplementary table S7. Dunnet's multiple-comparison post-test fitting the ANOVA with PI as the outcome variable.

ORCID

Marcelo M. Barreto Filho http://orcid.org/0000-0001-8392-5006
Pierre M. Durand http://orcid.org/0000-0002-9614-1371
Nathan E. Andolfato http://orcid.org/0000-0002-4812-6417
Anine Jordaan http://orcid.org/0000-0002-9093-790X
Hugo Sarmento http://orcid.org/0000-0001-5220-7992
Inessa L. Bagatini http://orcid.org/0000-0002-5549-2255

References

Affenzeller, M.J., Darehshouri, A., Andosch, A., Lutz, C. & Lütz-Meindl, U. (2009a). Salt stress-induced cell death in the unicellular green alga *Micrasterias denticulata*. *Journal of Experimental Botany*, **60**: 939–954.

Affenzeller, M.J., Darehshouri, A., Andosch, A., Lütz, C. & Lütz-Meindl, U. (2009b). PCD and autophagy in the unicellular green alga *Micrasterias denticulata*. *Autophagy*, **5**: 854–855.

Aravind, L. & Koonin, E.V. (2002). Classification of the caspase-hemoglobinase fold: detection of new families and implications for the origin of the eukaryotic separins. *Proteins Structural Functional Genetics*, **46**: 355–367.

Berges, J.A. & Choi, C.J. (2014). Cell death in algae: physiological processes and relationships with stress. *Perspectives in Phycology*, **1**: 103–112.

Berman-Frank, I., Bidle, K.D., Haramaty, L. & Falkowski, P.G. (2004). The demise of the marine cyanobacterium, *Trichodesmium* spp., via an autocatalyzed cell death pathway. *Limnology and Oceanography*, **49**: 997–1005.

Bidle, K.D. (2015). The molecular ecophysiology of programmed cell death in marine phytoplankton. *Annual Review of Marine Science*, **7**: 341–375.

Bidle, K.D. (2016). Programmed cell death in unicellular phytoplankton. *Current Biology*, **26**: R594–R607.

Bidle, K.D. & Falkowski, P.G. (2004). Cell death in planktonic, photosynthetic microorganisms. *Nature Reviews Microbiology*, **2**: 643–655.

Blackstone, N.W. (2016). An evolutionary framework for understanding the origin of eukaryotes. *Biology*, **5**: 18.

Blanca, M.J., Alarcón, R. & Arnau, J. (2017). Non-normal data: is ANOVA still a valid option? *Psicothema*, **29**: 552–557.

Bursch, W. (2001). The autophagosomal–lysosomal compartment in programmed cell death. *Cell Death and Differentiation*, **8**: 569–581.

Bursch, W., Ellinger, A., Gerner, Ch., Fröhwein, U. & Schulte-Hermann, R. (2006). Programmed cell death (PCD): apoptosis, autophagic PCD, or others? *Annals of the New York Academy of Sciences*, **926**: 1–12.

Carmona-Gutierrez, D., Bauer, M.A., Zimmermann, A., Aguilera, A., Austriaco, N., Ayscough, K., Balzan, R. *et al.* (2018). Guidelines and recommendations on yeast cell death nomenclature. *Microbial Cell,* **5**: 4–31. https://microbialcell.com/researcharticles/guidelines-and-recommendations-on-yeast-cell-death-nomenclature/

Carmona-Gutierrez, D., Eisenberg, T., Büttner, S., Meisinger, C., Kroemer, G. & Madeo, F. (2010). Apoptosis in yeast: triggers, pathways, subroutines. *Cell Death and Differentiation*, **17**: 763–773.

Carrión, C.A., Costa, M.L., Martínez, D.E., Mohr, C., Humbeck, K. & Guiamet, J.J. (2013). In vivo inhibition of cysteine proteases provides evidence for the involvement of 'senescence-associated vacuoles' in chloroplast protein degradation during dark-induced senescence of tobacco leaves, *Journal of Experimental Botany*, **64**: 4967–4980.

Cornillon, S., Foa, C., Davoust, J., Buonavista, N., Gross, J.D. & Golstein, P. (1994). Programmed cell death in *Dictyostelium. Journal of Cell Science*, **107**: 2691–2704.

Costa, M.L., Martínez, D.E., Gomez, F.M., Carrión, C.A. & Guiamet, J.J. (2013). Chloroplast protein degradation: involvement of senescence-associated vacuoles. In *Plastid Development in Leaves during Growth and Senescence* (Biswal, B., Krupinska, K. & Biswal, U.C., editors). Springer Netherlands, Dordrecht.

Danon, A., Delorme, V., Mailhac, N. & Gallois, P. (2000). Plant programmed cell death: a common way to die. *Plant Physiology and Biochemistry*, **38**: 647–655.

Dehning, I. & Tilzer, M.M. (1989). Survival of *Scenedesmus acuminatus* (Chlorophyceae) in darkness.*Journal of Phycol*ogy, **25**: 509–515.

Dingman, J.E. & Lawrence, J.E. (2012). Heat-stress-induced programmed cell death in *Heterosigma akashiwo* (Raphidophyceae). *Harmful Algae*, **16**: 108–116.

Durand, P.M. 2020. *The Evolutionary Origins of Life and Death*. Chicago, IL: University of Chicago Press.

Durand, P.M., Barreto Filho, M.M. & Michod, R.E. (2019). Cell death in evolutionary transitions in individuality. *Yale Journal of Biology and Medicine*, **92**: 651–662.

Durand, P.M., Choudhury, R., Rashidi, A. & Michod, R.E. (2014). Programmed death in a unicellular organism has species-specific fitness effects. *Biology Letters*, **10**: 20131088–20131088.

Durand, P.M. & Ramsey, G. (2019). The nature of programmed cell death. *Biological Theory*, **14**: 30–41.

Durand, P.M., Rashidi, A. & Michod, R.E. (2011). How an organism dies affects the fitness of its neighbors. *The American Naturalist*, **177**: 224–232.

Durand, P.M., Sym,S. & Michod, R.E. (2016). Programmed cell death and complexity in microbial systems. *Current Biology*, **26**: R587–R593.

Duszenko, M., Ginger, M.L., Brennand, A., Gualdrón-López, M., Colombo, M.I., Coombs, G.H., Coppens, I., Jayabalasingham, B., Langsley, G., Lisboa de Castro, S., Menna-Barreto, R., Mottram, J.C., Navarro, M., Rigden, D.J., Romano, P.S., Stoka, V., Turk, B. & Michels, P.A.M. (2011). Autophagy in protists. *Autophagy*, **7**: 127–158.

Eisenberg-Lerner, A., Bialik, S., Simon, H.-U. & Kimchi, A. (2009). Life and death partners: apoptosis, autophagy and the cross-talk between them. *Cell Death and Differentiation*, **16**: 966–975.

Franklin, D.J. & Berges, J.A. (2004). Mortality in cultures of the dinoflagellate Amphidinium carterae during culture senescence and darkness. *Proceedings of the Royal Society B: Biological Sciences*, **271**: 2099–107.

Franklin, D.J., Brussaard, C.P.D. & Berges, J.A. (2006). What is the role and nature of programmed cell death in phytoplankton ecology? *European Journal of Phycology*, **41**: 1–14.

Galluzzi, L., Vitale, I., Abrams, J.M., Alnemri, E.S., Baehrecke, E.H., Blagosklonny, T.M., Dawson, V.L., El-Deiry, W.S., Fulda, S., Gottlieb, E., Green, D.R., Hengartner, M.O., Kepp, O., Knight, R.A., Kumar, S., Lipton, S., Lu, X., Madeo, F., Malomi, W., Mehlen, P., Nunez, G., Peter, M.E., Piacentini, M., Rubinsztein, D.C., Shi, Y., Simon, H.U., Vandenabeele, P., White, E., Yuan, J., Zhivotovsky, B., Melino, G. & Kroemer, G. (2012). Molecular definitions of cell death subroutines: recommendations of the Nomenclature Committee on Cell Death 2012. *Cell Death and Differentiation*, **19**: 107–120.

Garcia da Silva, T., Bock, C., Sant'Anna, C.L., Bagatini, I.L., Wodniok, S. & Vieira, A.A.H. (2017). Selenastraceae (Sphaeropleales, Chlorophyceae): *rbc*L, 18S rDNA and ITS-2 secondary structure enlightens traditional taxonomy, with description of two new genera, *Messastrum* gen. nov. and *Curvastrum* gen. nov. *Fottea*, **17**: 1–19.

Gasol, J.M. & Morán, X.A.G. (2015). Flow cytometric determination of microbial abundances and its use to obtain indices of community structure and relative activity. In *Hydrocarbon and Lipid Microbiology Protocols* (McGenity, T.J., Timmis, K.N. & Nogales, B., editors), 159–187. Springer, Berlin.

Giroud, C., Gerber, A. & Eichenberger, W. (1988). Lipids of *Chlamydomonas reinhardtii*: analysis of molecular species and intracellular site(s) of biosynthesis. *Plant and Cell Physiology*, **29**: 587–595.

Gomes, L.C., Benedetto, G.D. & Scorrano, L. (2011). During autophagy mitochondria elongate, are spared from degradation and sustain cell viability. *Nature Cell Biology*, **13**: 589–598.

Gomes, L.C. & Scorrano, L. (2011). Mitochondrial elongation during autophagy: a stereotypical response to survive in difficult times. *Autophagy*, **7**: 1251–1253.

Griffiths, M.J., Garcin, C., van Hille, R.P. & Harrison, S.T. (2011). Interference by pigment in the estimation of microalgal biomass concentration by optical density, *Journal of Microbiological Methods*, **85**: 119–123.

Guillard, R.R.L. & Lorenzen, C.J. (1972). Yellow-green algae with chlorophyllide c^2. *Journal of Phycology*, **8**: 10–14.

Guiry, M.D. & Guiry, G.M. (2020). AlgaeBase. World-Wide Electronic Publication. National University of Ireland, Galway, 2020. http://www.algaebase.org

Hara-Nishimura, I. & Hatsugai, N. (2011). The role of vacuole in plant cell death. *Cell Death Differentiation*, **18**: 1298–1304.

Henics, T. & Wheatley, D.N. (1999). Cytoplasmic vacuolation, adaptation and cell death: a view on new perspectives and features. *Biology of the Cell*, **91**: 485–498.

Hofius, D., Munch, D., Bressendorff, S., Mundy, J. & Petersen, M. (2011). Role of autophagy in disease

resistance and hypersensitive response-associated cell death. *Cell Death Differentiation*, 18: 1257–1262.

Hothorn, T., Bretz, F. & Westfall P. (2008). Simultaneous inference in general parametric models. *Biometrical Journal*, 50: 346–363.

Hou, L., Liu, K., Li, Y., Ma, S., Ji, X. & Liu, L. (2016). Necrotic pyknosis is a morphologically and biochemically distinct event from apoptotic pyknosis. *Journal of Cell Science*, 129: 3084–3090.

Jiménez, C., Capasso, J.M., Edelstein, C.L., Rivard, C.J., Lucia, S., Breusegem, S., Berl, T. & Segovia, M. (2009). Different ways to die: cell death modes of the unicellular chlorophyte *Dunaliella viridis* exposed to various environmental stresses are mediated by the caspase-like activity DEVDase. *Journal of Experimental Botany*, 60: 815–828.

Jones, A.M. (2001). Programmed cell death in development and defense. *Plant physiology*, 125: 94–97.

Kay, P., Choudhury, R., Nel, M., Orellana, M.V. & Durand, P.M. (2013). Multicolour flow cytometry analyses and autofluorescence in chlorophytes: lessons from programmed cell death studies in *Chlamydomonas reinhardtii*. *Journal of Applied Phycology*, 25: 1473–1482.

Kol, E. & Flint, E.A. (1968) Algae in green ice from the Balleny Islands, Antarctica. *New Zealand Journal of Botany*, 6:3, 249–261.

Kozik, C., Young, E.B., Sandgren, C.D. & Berges, J.A. (2019). Cell death in individual freshwater phytoplankton species: relationships with population dynamics and environmental factors. *European Journal of Phycology*, 54: 369–379.

Krienitz, L. & Bock, C. (2012). Present state of the systematics of planktonic coccoid green algae of inland waters. *Hydrobiologia*, 698: 295–326.

Kroemer, G., Galluzzi, L., Vandenabeele, P., Abrams, J., Alnemri, E.S., Baehrecke, E. H., Blagosklonny, M.V., El-Deiry, W.S., Golstein, P., Green, D.R., Hengartner, M., Knight, R.A., Kumar, S., Lipton, S.A., Malorni, W., Nuñez, G., Peter, M. E., Tschopp, J., Yuan, J., Piacentini, M., Zhivotovsky, B. & Melino, G. (2009). Classification of cell death: recommendations of the Nomenclature Committee on Cell Death 2009. *Cell Death and Differentiation*, 16: 3–11.

Kurusu, T. & Kuchitsu, K. (2017). Autophagy, programmed cell death and reactive oxygen species in sexual reproduction in plants. *Journal of Plant Research*, 130: 491–499.

La Rocca, N., Sciuto, K., Meneghesso, A., Moro, I., Rascio, N. and Morosinotto, T. (2015). Photosynthesis in extreme environments: responses to different light regimes in the Antarctic alga *Koliella antarctica*. *Physiologia Plantarum*, 153 (4): 654–667.

Leist, M. & Nicotera, P. (1997). The shape of cell death. *Biochemical and Biophysical Research Communications*, 236: 1–9.

Leliaert, F., Smith, D.R., Moreau, H., Herron, M.D., Verbruggen, H., Delwiche, C.F. & De Clerck, O. (2012). Phylogeny and molecular evolution of the green algae. *Critical Reviews in Plant Sciences*, 31: 1–46.

Leu, K.-L., & Hsu, B.-D. (2005). A programmed cell disintegration of *Chlorella* after heat stress. *Plant Science*, 168: 145–152.

Lewis, L.A. & McCourt, R.M. (2004). Green algae and the origin of land plants. *American Journal of Botany*, 91: 1535–1556.

Lockshin, R.A. & Williams, C.M. (1964). Programmed cell death–II. Endocrine potentiation of the breakdown of the intersegmental muscles of silk moths. *Journal of Insect Physiology*, 10: 643–649.

Lockshin R.A. & Zakeri, Z. (2004). Apoptosis, autophagy, and more. *International Journal of Biochemistry and Cell Biology*, 36: 2405–2419.

Maiuri, M.C., Zalckvar, E., Kimchi, A. & Kroemer, G. (2007). Self-eating and self-killing: crosstalk between autophagy and apoptosis. *Nature Reviews Molecular Cell Biology*, 8: 741–752.

Mata, M.T., Palma, A., García-Gómez, C., López-Parages, M., Vázquez, V., Cheng-Sánchez, I., Sarabia, F; López-Figueroa, F., Jiménez, C. & Segovia, M. (2019). Type II-Metacaspases are involved in cell stress but not in cell death in the unicellular green alga *Dunaliella tertiolecta*. *Microbial Cell*, 6: 494–508.

Michod, R.E. & Nedelcu, A.M. (2003). On the reorganization of fitness during evolutionary transitions in individuality. *Integrative and Comparative Biology*, 43: 64–73.

Minina, E. A., Smertenko, A.P. & Bozhkov, P.V. (2014b). Vacuolar cell death in plants: Metacaspase releases the brakes on autophagy. *Autophagy*, 10: 928–929.

Minina, E.A., Bozhkov, P.V. & Hofius, D. (2014a). Autophagy as initiator or executioner of cell death. *Trends in Plant Science*, 19: 692–697.

Minina, E.A., Coll, N.S., Tuominen, H. & Bozhkov, P.V. (2017). Metacaspases versus caspases in development and cell fate regulation. *Cell Death Differentiation*, 24: 1314–1325.

Minina, E.A., Filonova, L.H., Fukada, K., Savenkov, E.I., Gogvadze, V., Clapham, D., Sanchez-Vera, V. et al. (2013). Autophagy and metacaspase determine the mode of cell death in plants. *Journal of Cell Biology*, 203: 917–927.

Minina, E.A., Staal, J., Alvarez, V.E., Berges, J.Á., Berman-Frank, I., Beyaert, R., Bidle K.D., Bornancin, F., Casanova, M., Cazzulo, J.J., Choi, C.J., Coll, N.S., Dixit, V. M., Dolinar, M., Fasel, N., Funk, C., Gallois, P., Gevaert, K., Gutierrez-Beltran, E., Hailfinger, S., Klemenčič, M., Koonin, E.V., Krappmann, D., Linusson, A., Machado, M. F.M., Madeo, F., Megeney, L.A., Moschou, P.N., Mottram, J. C., Nyström, T., Osiewacz, H.D., Overall, CM., Pandey, K. C., Ruland, J., Salvesen, G.S., Shi, Y., Smertenko, A., Stael, S., Ståhlberg, J., Suárez, M.F., Thome, M., Tuominen, H., Van Breusegem, F., van der Hoorn, R.A.L., Vardi, A., Zhivotovsky, B., Lam, E. & Bozhkov P.V. (2020). Classification and nomenclature of metacaspases and paracaspases: no more confusion with caspases. *Molecular Cell*, 77: 927–929.

Moharikar, S., D'Souza, J.S., Kulkarni, A.B. & Rao, B.J. (2006). Apoptotic-like cell death pathway is induced in unicellular chlorophyte *Chlamydomonas reinhardtii* (chlorophyceae) cells following UV irradiation: detection and functional analyses. *Journal of Phycology*, 42: 423–433.

Murik, O., Elboher, A. & Kaplan, A. (2014). Dehydroascorbate: a possible surveillance molecule of oxidative stress and programmed cell death in the green alga *Chlamydomonas reinhardtii*. *New Phytologist*, 202: 471–84.

Murik, O. & Kaplan, A. (2009). Paradoxically, prior acquisition of antioxidant activity enhances oxidative stress-induced cell death. *Environmental Microbiology*, 11: 2301–9.

Nedelcu, A.M. (2006). Evidence for p53-like-mediated stress responses in green algae. *FEBS Letters*, 580: 3013–3017.

Nedelcu, A.M., Driscoll, W.W., Durand, P.M., Herron, M. D. & Rashidi, A. (2011). On the paradigm of altruistic suicide in the unicellular world. *Evolution*, **65**: 3–20.

Nedelcu, A.M., Marcu, O. & Michod, R.E. (2004). Sex as a response to oxidative stress: a twofold increase in cellular reactive oxygen species activates sex genes. *Proceedings of the Royal Society of London. Series B: Biological Sciences*, **271**: 1591–1596.

Ning, S.-B., Guo, H.-L., Wang, L. & Song, Y.-C. (2002). Salt stress induces programmed cell death in prokaryotic organism *Anabaena*. *Journal of Applied Microbiology*, **93**: 15–28.

Nozaki, H., Kuroiwa, H. & Kuroiwa, T. (1994). Light and electron microscopic characterization of two types of pyrenoids in *Gonium* (Goniaceae, Chlorophyta). *Journal of Phycology*, **30**: 279–290.

Orellana, M.V., Pang, W.L., Durand, P.M., Whitehead, K. & Baliga, N.S. (2013). A role for programmed cell death in the microbial loop. *PLoS ONE*, **8**: e62595.

Otto, G.P., Wu, M.Y., Kazgan, N., Anderson, O.R. & Kessin, R. H. (2003). Macroautophagy is required for multicellular development of the social amoeba *Dictyostelium discoideum*. *Journal of Biological Chemistry*, **278**: 17636–17645.

Papini, A., Gonnelli, C., Tani, C., Falco, P.D., Wolswijk, G., Santosuosso, U., Nuccio, C. *et al.* (2018). Autophagy induced by heavy metal and starvation stress in microalgae. *Phytomorphology*, **68**: 7–12.

Philipps, G., Happe, T. & Hemschemeier, A. (2012). Nitrogen deprivation results in photosynthetic hydrogen production in *Chlamydomonas reinhardtii*. *Planta*, **235**: 729–745.

Proto, W.R., Coombs, G.H. & Mottram, J.C. (2013). Cell death in parasitic protozoa: regulated or incidental? *Nature Reviews Microbiology*, **11**: 58–66.

Reynolds, E.S. (1963). The use of lead citrate at high pH as an electron-opaque stain in electron microscopy. *Journal of Cell Biology*, **17**: 208–212.

Sathe, S., Orellana, M.V., Baliga, N.S. & Durand, P. M. (2019). Temporal and metabolic overlap between lipid accumulation and programmed cell death due to nitrogen starvation in the unicellular chlorophyte *Chlamydomonas reinhardtii*. *Phycological Research*, **67**: 173–183.

Satpati, G.G., Gorain, P.C. & Pal, R. 2016. Efficacy of EDTA and phosphorous on biomass yield and total lipid accumulation in two green microalgae with special emphasis on neutral lipid detection by flow cytometry. *Advances in Biology*, **2016**: ID 8712470.

Saunders, J.W. (1966). Death in embryonic systems. *Science*, **154**: 604–612.

Segovia, M. & Berges, J. A. (2009). Inhibition of caspase-like activities prevents the appearance of reactive oxygen species and dark-induced apoptosis in the unicellular chlorophyte *Dunaliella tertiolecta*. *Journal of Phycology*, **45**: 1116–1126.

Segovia, M., Haramaty, L., Berges, J.A. & Falkowski, P.G. (2003). Cell death in the unicellular chlorophyte *Dunaliella tertiolecta*: a hypothesis on the evolution of apoptosis in higher plants and metazoans. *Plant Physiology*, **132**: 99–105.

Sperandio, S., de Belle, I. & Bredesen, D.E. (2000). An alternative, nonapoptotic form of programmed cell death. *Proceedings of the National Academy of Sciences USA*, **97**: 14376–14381.

Spungin, D., Bidle, K.D. & Berman-Frank, I. (2019). Metacaspase involvement in programmed cell death of the marine cyanobacterium *Trichodesmium*. *Environmental Microbiology* **21**: 667–681.

Tischner, R., Heise, K.-P., Nelle, R. & Lorenzen, H. (1978). Changes in pigment content, lipid pattern and ultrastructure of synchronous *Chlorella* after heat and cold shocks. *Planta*, **139**: 29–33.

Tsiatsiani, L., Van Breusegem, F., Gallois, P., Zavialov, A., Lam, E. & Bozhkov, P.V. (2011). Metacaspases. *Cell Death and Differentiation*, **18**: 1279–1288.

Tsujimoto, Y. & Shimizu, S. (2005). Another way to die: autophagic programmed cell death. *Cell Death and Differentiation*, **12**: 1528–1534.

Uren, A.G., O'Rourke, K., Aravind, L., Pisabarro, M.T., Seshagiri, S., Koonin, E.V. & Dixit, V.M. (2000). Identification of paracaspases and metacaspases two ancient families of caspase-like proteins, one of which plays a key role in MALT lymphoma. *Molecular Cell*, **6**: 961–967.

van Doorn, W.G., Beers, E.P., Dangl, J.L., Franklin-Tong, V.E., Gallois, P., Hara-Nishimura, I., Jones, A.M., Kawai-Yamada, M., Lam, E., Mundy, J., Mur, L.A.J., Petersen, M., Smertenko, A., Taliansky, M., Van Breusegem, F., Wolpert, T., Woltering, E., Zhivotovsky, B. & Bozhkov, P. V. (2011). Morphological classification of plant cell deaths. *Cell Death and Differentiation*, **18**: 1241–1246.

Vardi, A. (2008). Cell signaling in marine diatoms. *Communicative and Integrative Biology*, **1**: 134–136.

Vardi, A., Eisenstadt, D., Murik, O., Berman-Frank, I., Zohary, T., Levine, A. & Kaplan, A. (2007). Synchronization of cell death in a dinoflagellate population is mediated by an excreted thiol protease. *Environmental Microbiology*, **9**: 360–369.

Vavilala, S.L., Gawde, K.K., Sinha, M. & D'Souza, J.S. (2015). Programmed cell death is induced by hydrogen peroxide but not by excessive ionic stress of sodium chloride in the unicellular green alga *Chlamydomonas reinhardtii*. *European Journal Phycology*, **50**: 422–38.

Vavilala, S.L., Sinha, M. & D'Souza, J.S. (2014). Menadione-induced caspase-dependent programmed cell death in the green chlorophyte *Chlamydomonas reinhardtii*. *Journal of Phycology*, **50**: 587–601.

Weingärtner, A., Kemmer, G., Müller, F.D., Zampieri, R.A., Gonzaga dos Santos, M., Schiller, J. & Pomorski, T.G. (2012). Leishmania promastigotes lack phosphatidylserine but bind annexin V upon permeabilization or miltefosine treatment. *PLoS ONE*, **7**: e42070.

Wickham, H., Averick, M., Bryan, J., Chang, W., McGowan, L., François, R., Grolemund, G. *et al.* (2019). Welcome to the Tidyverse. *Journal of Open Source Software*, **4**: 1686.

Yordanova, Z.P., Woltering, E.J., Kapchina-Toteva, V.M. & Iakimova, E.T. (2013). Mastoparan-induced programmed cell death in the unicellular alga *Chlamydomonas reinhardtii*. *Annals of Botany*, **111**: 191–205.

Zargar, S., Krishnamurthi, K., Devi, S.S., Ghosh, T.K. & Chakrabarti (2006). Temperature-induced stress on growth and expression of hsp in freshwater alga *Scenedesmus quadricauda*. *Biomedical and Environmenal Sciences*, **19**: 414–421.

Zhou, T., Cao, H., Zheng, J., Teng, F., Wang, X., Lou, K., Zhang, X. & Tao, Y. (2020). Suppression of water-bloom cyanobacterium *Microcystis aeruginosa* by algaecide hydrogen peroxide maximized through programmed cell death. *Journal of Hazardous Materials*, **393**: 122–394.

Zuppini, A., Andreoli, C. & Baldan, B. (2007). Heat stress: an inducer of programmed cell death in *Chlorella saccharophila*. *Plant and Cell Physiology*, **48**: 1000–1009.